Considering Symmetry Properties of InP Nanowire/Light Incidence Systems to Gain Broadband Absorption
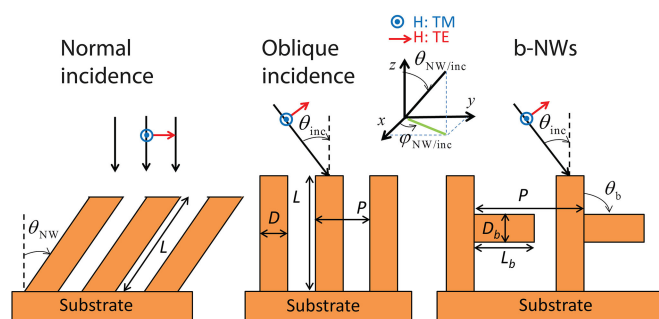
Mahtab Aghaeipour
Mats-Erik Pistol
Hakan Pettersson

Considering Symmetry Properties of InP Nanowire/Light Incidence Systems to Gain Broadband Absorption

Mahtab Aghaeipour,[1] **Mats-Erik Pistol,**[1] **and Hakan Pettersson**[1,2]

[1]Solid State Physics and NanoLund, Lund University, Lund 22100, Sweden
[2]Department of Mathematics, Physics and Electrical Engineering, Halmstad University, Halmstad SE-301 18, Sweden

Abstract: Geometrically designed III-V nanowire arrays are promising candidates for disruptive optoelectronics due to the possibility of obtaining a strongly enhanced absorption resulting from nanophotonic resonance effects. With normally incident light on such vertical nanowire arrays, the absorption spectra exhibit peaks that originate from excitation of HE_{1m} waveguide modes in the constituent nanowires. However, the absorption spectra typically show dips between the absorption peaks. Conventionally, such weak absorption has been counteracted by either making the nanowires longer or by decreasing the pitch of the array, both alternatives effectively increasing the volume of absorbing material in the array. Here, we first study two approaches for compensating the absorption dips by exciting additional Mie resonances: 1) oblique light incidence on vertical InP nanowire arrays and 2) normal light incidence on inclined InP nanowire arrays. We then show that branched nanowires offer a novel route to achieve broadband absorption by taking advantage of simultaneous excitations of Mie resonances in the branches and guided HE_{1m} modes in the stem. Finite element method calculations show that the absorption efficiency is enhanced from 0.72 for vertical nanowires to 0.78 for branched nanowires under normal light incidence. Our work provides new insight for the development of novel efficient photovoltaics with high efficiency and reduced active material volume.

Index Terms: Nanophotonics, nanowire arrays, absorption, guided modes, Mie resonances, photovoltaics.

1. Introduction

Over the last two decades, there has been a dramatic increase in research activities related to nanowires (NWs) due to their exciting prospects for implementation of novel high-performance transistors [1], LEDs [2], lasers [3], photodetectors [4], [5], and sensors [6] compatible with main-stream silicon technology. The exact geometry of NWs plays a crucial role in many photonic applications, e.g., photodetectors and solar cells, where strong absorption resonances can be obtained by proper tailoring of NW diameter, length and pitch [7]–[11]. However, the absorption efficiency of NW-based solar cells is still limited in the solar spectrum by insufficient absorption at wavelengths between spectrally fairly separated resonance modes. Conventional approaches to circumvent this prob-

lem typically aim at increasing the amount of absorbing material in the array, e.g., by decreasing (increasing) the NW pitch (length). Here, we propose alternative strategies to enhance the absorption by breaking the symmetry of the NW array/light incidence system, fundamentally underlying the resonance modes observed for vertical arrays in combination with normal incident light.

Absorption spectra of NWs display peaks at wavelengths where the incident light strongly excites optical modes with high extinction coefficient (the imaginary part of the refractive index) [12]–[15]. To improve the absorption at a particular wavelength, two basic requirements thus have to be met: the incident light must excite the mode at the target wavelength and the excited mode has to be strongly absorbed in the NWs [15]. A lot of studies investigate tailoring of the absorption properties of semiconductor NWs [13], [16]–[22] in terms of geometrical parameters, but still the absorption spectra exhibit performance-limiting dips. Since these dips are related to the symmetry of the NW array/light incidence system, in-depth studies of symmetry-breaking oblique excitation should be carried out. Such oblique conditions can be realized for example by either normal incidence excitation of inclined NWs [23]–[25] or by oblique excitation of vertically standing NWs [12], [26]. Recently, enhanced absorption was reported for both GaAs NWs [27] and InP NWs [28] when increasing the oblique incidence angle up to 45°. Here we theoretically study absorption efficiency of InP NWs under oblique conditions and calculate comparative absorption spectra for different broken symmetry cases. In particular, we show that oblique incident light on vertical NW arrays improves the integrated absorption efficiency compared to inclined NW arrays and normal incident light. The oblique conditions, however, enhances the absorption of Mie resonances [26], [29] at the expense of reduced excitation of guided modes [29]. The ultimate goal would be to obtain an unselective absorption in a broad range of the solar spectrum. To realize this we propose to utilize branched NWs (b-NWs) [30] comprising both a conventional NW stem and a connected branch, offering simultaneous excitation of strong Mie resonances in the branches and guided modes in the stems. Moreover, the b-NW arrays offer several advantages for high-efficiency photovoltaic applications compared to conventional NW arrays due to a stepwise growth method [31] where crystal structure, material system, and geometrical parameters can be changed in three directions [30]. By comparing the calculated absorption efficiency in NWs under oblique conditions with b-NWs we demonstrate a significant enhancement in absorption over a broad spectral range by taking simultaneous advantage of exciting Mie resonances (in the branch) and guided modes (in the stem). Due to preferred omnidirectional absorption in solar cells, b-NWs are promising building blocks for high performance NW based solar cells. In this work we have investigated InP NWs, but we believe that our conclusions are valid also for other direct bandgap semiconductor material systems.

2. Calculations

To calculate absorption spectra for NW arrays, we employed a finite element method (COMSOL software package) and solved Maxwell's equations using tabulated data for the refractive index of InP [32]. We use a full-field electromagnetic wave solver in the Multiphysics module to find the electric field distribution inside and outside the NWs under plane wave incidence. The calculations are carried out for wavelengths ranging from 300 nm to 1000 nm, in 10 nm steps. We use perfectly matched layer (PML) boundary conditions in the vertical z-direction and Floquet boundary conditions in the x- and y-direction to construct an infinite periodic square array. We take the volume integral of the power loss density over the NWs to calculate the absorption spectra. Here, we calculate the absorption spectra for sparse square NW arrays. Since the optical absorption of sparse NW arrays does not depend strongly on the lattice arrangement [33], we believe that the results are valid to a good approximation for other arrangements, like, e.g., hexagonal arrays. Fig. 1 shows schematics of the considered asymmetric NW array/light incidence systems. The NWs are assumed to be grown on an InP substrate. The upper insets display the geometry of the transverse magnetic (TM) and the transverse electric (TE) polarized light. The TM (TE) modes are characterized by a magnetic field vector polarized perpendicular (parallel) to the plane of incidence, i.e., the x-z plane with $\varphi_{inc} = 0°$. Correspondingly, we define the orientation of the NWs by the azimuthal angle φ_{NW}. The geometrical properties considered for the square arrays of the NWs are the diameter D, length L, branch diameter D_b, branch length L_b, and distance P between the NWs, i.e., the array pitch. The polar angles θ_{inc},
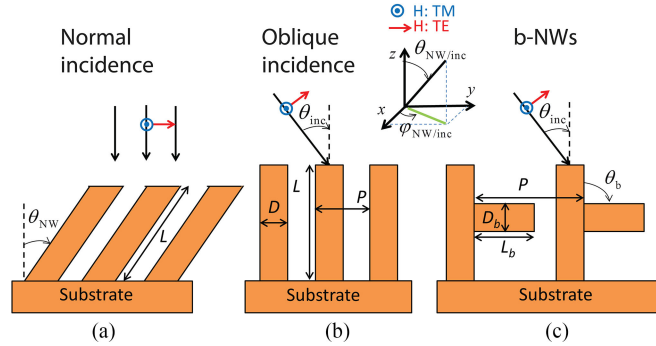
Fig. 1. Schematics of the considered NW array/light incidence systems. The insets in the upper panel show the spherical coordinate system together with defined H polarization vectors of the TM and TE modes in the plane of incidence (x-z plane). $\varphi_{NW}/\varphi_{inc}$ defines the azimuthal orientation of NWs and the light, respectively. (a) Inclined NWs (θ_{NW}, $\varphi_{NW} = 0°$) and normal incident light ($\theta_{inc} = 0°$, $\varphi_{inc} = 0°$). (b) Vertical NWs ($\theta_{NW} = 0°$, $\varphi_{NW} = 0°$) and oblique incident light (θ_{inc}, $\varphi_{inc} = 0°$). (c) b-NWs ($\theta_{NW} = 0°$, $\theta_b = 90°$, $\varphi_{NW} = 0°$) and oblique incident light (θ_{inc}, $\varphi_{inc} = 0°$).

θ_{NW} and θ_b represent the angle between the oblique incident light and vertical NWs, the angle between the substrate normal and the axis of inclined NWs and the angle between NW and branch, respectively, as shown in Fig. 1. In the calculations, we set $\varphi_{NW} = 0$ due to the expected weak φ-dependence in the absorption properties of square NW arrays [34]. This assumption is corroborated by calculations of absorption spectra for different values of φ_{NW} shown in the Appendix (see Fig. 9).

To evaluate the absorption characteristics of the NWs in the solar spectrum, we use the (normalized) absorption efficiency η, which is defined as

$$\eta = \frac{\int_{300}^{920} I(\lambda) A(\lambda) \frac{\lambda}{\lambda_g} d\lambda}{\int_{300}^{920} I(\lambda) \frac{\lambda}{\lambda_g} d\lambda} \tag{1}$$

where λ is the photon wavelength, and λ_g is the photon wavelength corresponding to the band gap of InP. Here, $A(\lambda)$ is the absorption of the NW array, that is, the fraction of incident light that is absorbed in the NWs at wavelength λ. $I(\lambda)$ is the solar spectral irradiance assuming standard air mass 1.5 (AM1.5) [35]. We chose the spectral range from 300 nm to 920 nm in the integration due to the band gap of InP (1.344 eV, 920 nm), and the fact that $I(\lambda)$ is negligible for $\lambda < 300$ nm.

3. Results and Discussions

An asymmetric system ($\theta_{inc} \neq 0°$ or $\theta_{NW} \neq 0°$) is expected to exhibit polarized absorption characteristics. We first investigate the absorption spectra resulting from normally incident light on inclined NW arrays (Fig. 1(a)). To compare these results with the corresponding spectra of vertical NW arrays ($\theta_{NW} = 0$), we average the TM and TE absorption spectra and denote the resulting spectrum the *polarization-averaged* spectrum.

Fig. 2 shows the calculated absorption spectra of inclined InP NWs as a function of θ_{NW} and diameter D for a given length $L = 1100$ nm and pitch $P = 500$ nm when the incident light is normal ($\theta_{inc} = 0$). We chose these geometrical parameters since they allow an analysis of the θ_{NW}-dependence with no signs of absorption saturation that can be observed for longer NWs [21], [36] or denser arrays (smaller pitch) of NWs [10] (see Fig. 10 in the appendix). Each panel includes the absorption spectrum in green color of vertical NW arrays ($\theta_{NW} = 0$) for comparison. When increasing θ_{NW}, the results confirm an enhanced absorption in inclined NWs, compared to vertical arrays, in the middle part of the spectrum at wavelengths in between resonant HE_{1m} modes (m is the radial mode number). We point out that only HE_{1m} modes lead to absorption peaks in vertical NW arrays [16], [37] due to the symmetry requirements. As the diameter decreases from 200 nm (see Fig. 2(a)) to 50 nm (see Fig. 2(d)), the absorption in general decreases and becomes increasingly polarization dependent [23]. For inclined NWs with $D = 50$ nm and $\theta_{NW} > 45°$, the guided HE_{1m}
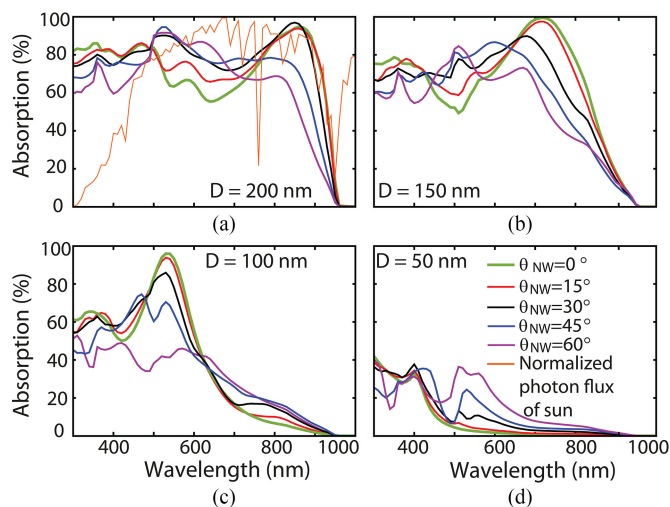
Fig. 2. Polarization-averaged absorption spectra of inclined InP NWs of varying D (200, 150, 100, and 50 nm) and constant $L = 1100$ nm and $P = 500$ nm. The incident light is normal to the substrate. Each panel includes the absorption spectrum of the corresponding vertical NW array $\theta_{NW} = 0$ (green curve). The normalized solar photon flux (orange curve) is shown in (a).
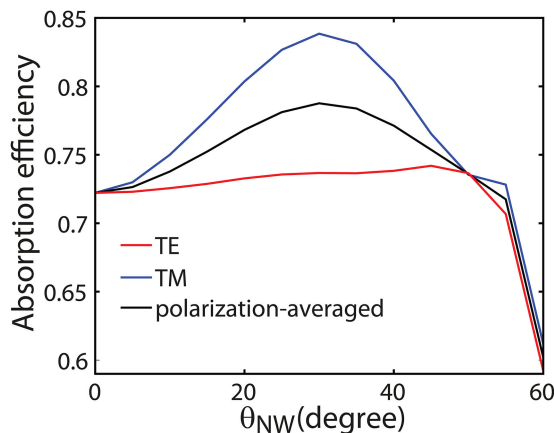

Fig. 3. Normalized TM, TE, and polarization-averaged absorption efficiency of inclined InP NWs for $D = 200$ nm, $L = 1100$ nm, and $P = 500$ nm versus inclination angle. The incident light is normal to the substrate ($\theta_{inc} = 0°$). $\theta_{NW} = 0°$ corresponds to vertical NWs for which the absorption is independent of polarization.

modes are limited to the short-wavelength regime and a significant contribution is instead obtained from Mie resonances at longer wavelengths. Moreover, the TM absorption is considerably stronger (not shown here) than both the TE absorption and the polarization-averaged absorption of vertical NW arrays [4].

To stress the importance of the spectral range of the enhanced absorption, we plot the spectrum of the normalized solar photon flux, $I(\lambda)\frac{\lambda}{hc}$ (photons m^{-2} sec^{-1}) [35], in Fig. 2(a) (orange curve), where h is Planck's constant, and c is the speed of light in vacuum. It is observed that the spectral region of enhanced absorption matches the maximum photon flux from the sun particularly for inclined NWs with $D = 200$ nm and $\theta_{NW} = 30°$, which in turn is important for photovoltaic applications.

Thus, inclined NWs improve the absorption efficiency compared to vertical NWs for a limited range of inclination angles. To quantify this enhancement further, we employ Eq. (1) to calculate the absorption efficiency, η, for inclined NW arrays versus inclination angle (see Fig. 3). The blue curve shows that the absorption efficiency for in particular TM polarized light is significantly improved for all angles. The polarization-averaged absorption efficiency (black curve) becomes maximum at an
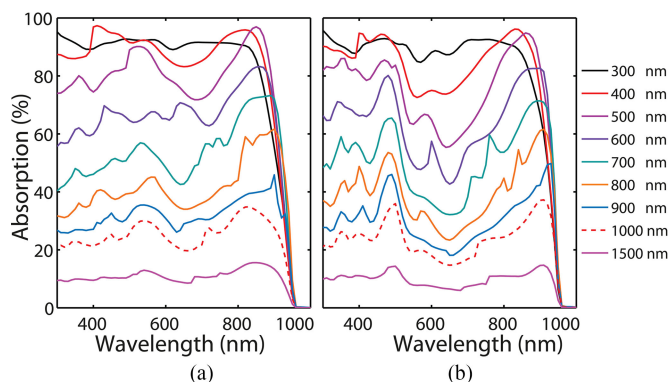
Fig. 4. Polarization-averaged absorption spectra versus pitch P for (a) inclined $\theta_{NW} = 30°$ and (b) vertical $\theta_{NW} = 0°$ InP NWs with $D = 200\,nm$ and $L = 1100\,nm$. The incident light is normal to the substrate ($\theta_{inc} = 0$). The considered values of P are shown to the right of (b).
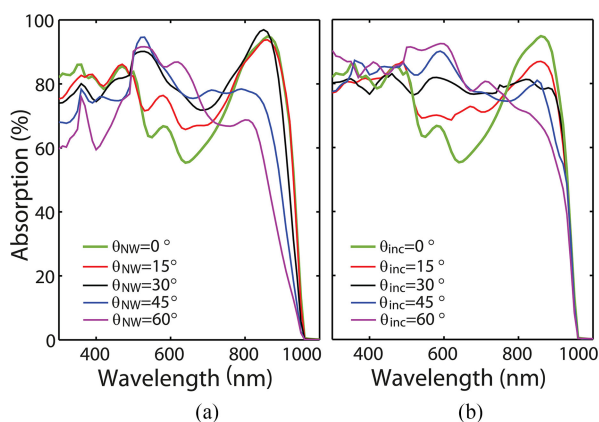

Fig. 5. Polarization-averaged absorption spectra for (a) inclined and (b) vertical NWs with identical dimensions ($D = 200\,nm$, $L = 1100\,nm$, and $P = 500\,nm$). The green curve shows the absorption spectrum for vertical NWs with the same geometrical parameters for normal incident light.

angle of about $\theta_{NW} = 30°$, which roughly corresponds to the natural inclination angle (35.5°) of InP NWs grown on (001) InP substrates. Fig. 3 furthermore shows that the absorption efficiency is significantly improved for all angles $\theta_{NW} < 45°$ compared to vertical NWs.

Fig. 4 depicts the influence of pitch P on the absorption spectra for 30° inclined NWs (see Fig. 4(a)) and vertical NWs (see Fig. 4(b)), respectively. This 30° inclination angle was chosen based on the observed maximum polarization-averaged absorption efficiency in Fig. 3 at $\theta_{NW} \approx 30°$. Fig. 4 shows that decreasing the pitch enhances the absorption at all wavelengths for both vertical and inclined NWs down to $P = 400\,nm$, below which the absorption drops and saturates. Positioning the NWs too close together furthermore causes broadening and eventually disappearing absorption resonances due to either coupling of the excited modes or saturation of the absorption for all wavelengths (like in a bulk system). At $P = 1500\,nm$, where the absorption spectrum can be attributed to a single NW rather than to an array, the results still show an enhanced absorption for inclined NWs. It should also be noted that inclined NWs exhibit enhanced absorption in the solar spectrum for all pitches compared to the symmetric vertical NW/normal incidence system.

The results for inclined NWs (see the schematics in Fig. 1(a)) discussed above pose the interesting question whether similar enhanced absorption is obtained for oblique incident light on vertical NW arrays (see schematics in Fig. 1(b)). Fig. 5 shows that the absorption characteristics of both asymmetric systems are enhanced in the middle part of the spectral range compared to the symmetric system ($\theta_{NW} = \theta_{inc} = 0$). Comparing the two asymmetric cases, it is evident that the
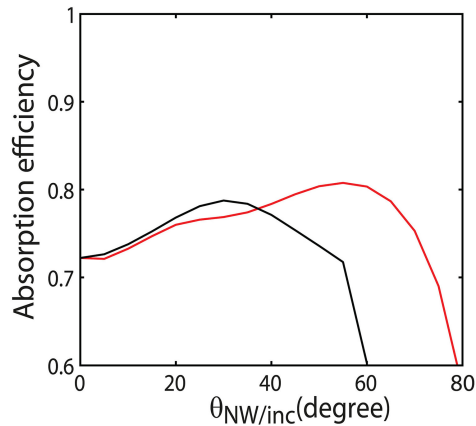
Fig. 6. Normalized polarization-averaged absorption efficiency for varying inclination angle θ_{NW} of inclined InP NWs at normal incidence (black curve) and varying incidence angle θ_{inc} for vertical NWs (red curve). The geometrical parameters of the NW arrays are identical ($D = 200$ nm, $L = 1100$ nm, and $P = 500$ nm).
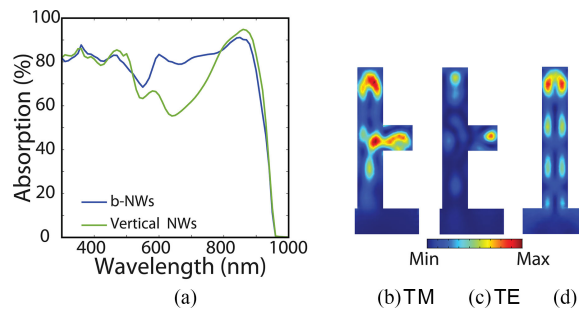

Fig. 7. (a) Polarization-averaged absorption spectra for b-NWs and vertical NWs, with dimensions $L = 1100$ nm, $D_b = 200$ nm, $L_b = 250$ nm, and $P = 500$ nm for normal incident light. (b)–(d) Photon absorption profiles.

absorption peaks decrease more significantly with increasing angle θ_{NW} for inclined NWs than with θ_{inc} for oblique light incidence on vertical NWs, especially at longer wavelengths.

To gain more insight into the difference between the absorption characteristics of both asymmetric systems, we calculated the polarization-averaged absorption efficiency using Eq. (1) (see Fig. 6). The results show an enhancement of the absorption efficiency for either asymmetric system compared to the symmetric system, with either $\theta_{NW} < 40°$ (with $\theta_{inc} = 0$) or $\theta_{inc} < 40°$ (with $\theta_{NW} = 0$). Moreover, the polarization-averaged absorption efficiency under oblique incidence conditions is significantly improved compared to both vertical NWs and inclined NWs for $40° < \theta_{NW/inc} < 55°$. Thus, breaking the symmetry of the NW array/incident light system is a way to achieve enhanced absorption efficiency. However, both oblique excitation conditions offer, as mentioned above, an enhanced absorption limited by the trade-off between excitation of Mie resonances at large θ_{inc}/θ_{NW} and guided HE_{1m} modes at $\theta_{inc}/\theta_{NW} = 0$.

The results above indicate that strong simultaneous excitation of both Mie resonances and guided modes is necessary to achieve a broadband absorption spectrum desired for photovoltaic applications. The b-NWs (see the schematics in Fig. 1(c)) allows for realizing such a broadband absorption spectrum under normal incident light. Fig. 7(a) shows a normal incidence absorption spectrum of b-NWs with $\theta_b = 90°$ expected for zinc-blende b-NWs ($\theta_b = 35.5°$ expected for wurtzite polytypes) to compare with vertical NWs. The growth of b-NWs is a stepwise method [31]. The branches can be grown in other materials and with different crystal structure and geometrical parameters than the main stem. In literature is typically reported that branches grow perpendicular to the stem, especially for wurtzite NWs [38], [39]. Another common case that can occur for
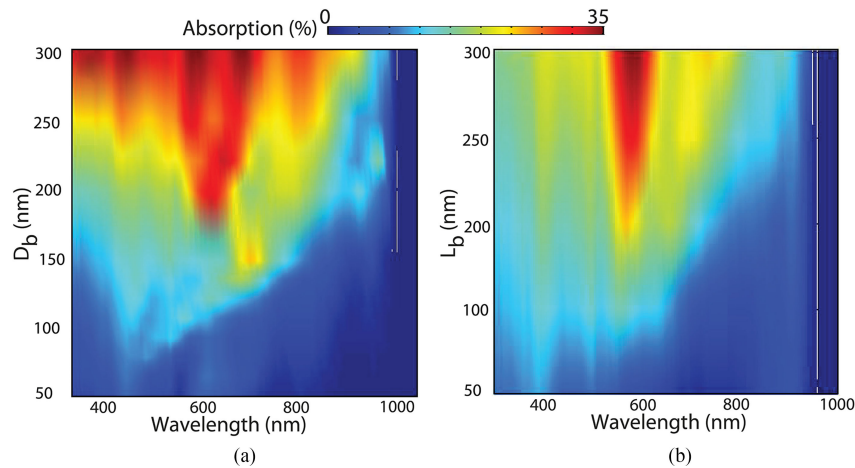
Fig. 8. (a) Polarization-averaged absorption spectra of the branches of b-NWs as a function of (a) the branch diameter D_b for a given length $L_b = 250$ nm and (b) the branch length L_b for a given diameter $D_b = 200$ nm for normal incident light. The pitch is constant ($P = 500$ nm). The color bar shows the optical absorption intensity.

zincblende NWs is that branches grow in symmetry-related <111> directions at an angle of 109° to the stem. Here we have chosen to focus on the common realistic case of perpendicular branches. The geometrical parameters for the InP b-NW arrays were chosen as $L = 1100$ nm, $L_b = 250$ nm, $D_b = 200$ nm and $P = 500$ nm. Adding a horizontal branch to the vertical NW (stem) excites Mie resonances in the branch at normal incidence and improves the absorption spectra significantly at the dips observed for vertical NWs without branches. Fig. 7(b)–(d) show the corresponding photon absorption profiles of TM and TE polarized light for the b-NW arrays, and of vertical NWs at a wavelength of 640 nm where the absorption spectrum of vertical NWs shows a dip (see the green trace in Fig. 7(a)). The simulations furthermore reveal the importance of optimizing the position of the branch along the stem (here 500 nm) to maximize the absorption in the b-NWs. Calculations show that for normal incident light, the absorption efficiency has enhanced from 0.72 for vertical NWs to 0.78 for the b-NWs.

To investigate the effect of the geometrical parameters of the branch on excited modes, we calculate the absorption in the branches of b-NWs at normal light incidence. Fig. 8 shows the polarization-averaged absorption spectra of the branch, excluding the absorption in the stem, as a function of diameter D_b (see Fig. 8(a)) and length L_b (see Fig. 8(b)) for a given pitch $P = 500$ nm. Increasing the geometrical dimensions of the branches show that strong Mie resonances appear in the middle range of the absorption spectrum where the absorption spectra of vertical NWs exhibit dips. Consequently, we expect well-designed b-NWs to display strong optical resonances in a broad spectral range due to simultaneous excitation and absorption of guided optical modes in the NW stems and Mie modes in the branches (see Fig. 7(a)).

4. Conclusion

In summary, we have theoretically investigated the absorption efficiency of asymmetric NW array/light incidence systems. Our results show the importance of taking into account symmetry properties when optimizing the absorption efficiency in light-harvesting NW devices. Compared to vertical NWs and normal light incidence, the absorption efficiency improves for both studied systems of inclined NWs and oblique light incidence due to enhanced absorption at wavelengths between the peaks caused by the HE_{1m} modes in vertical NW arrays at normal incidence. Furthermore, we show that a broadband absorption spectrum is achievable for b-NWs due to strong simultaneous excitation of both Mie resonances and HE_{1m} modes. The observed enhancement is significant in the part of the solar spectrum that exhibits high irradiance, which opens up promising routes to enhance the efficiency of solar cells by engineering the symmetry properties. In this work
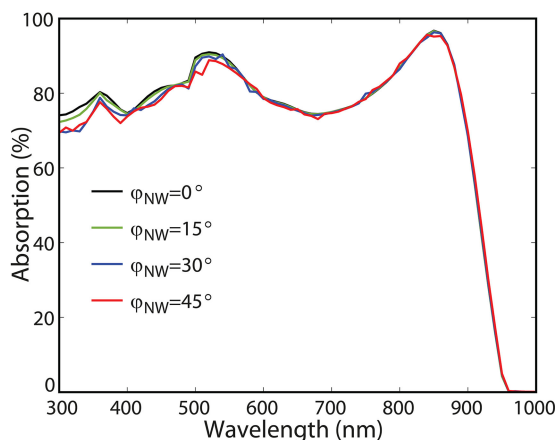
Fig. 9. Polarization-averaged absorption spectra under normal light excitation ($\theta_{inc} = 0°$, $\varphi_{inc} = 0°$) of inclined NWs as a function of φ_{NW}. The geometrical parameters of the NW arrays are $D = 200\,\text{nm}$, $L = 1100\,\text{nm}$, and $P = 500\,\text{nm}$.
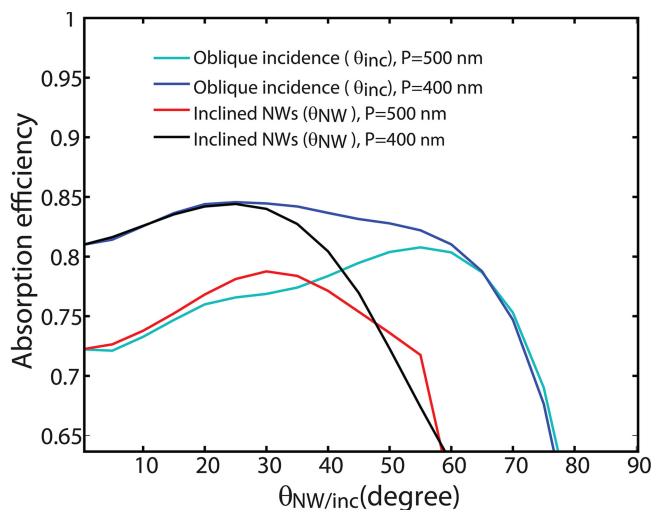

Fig. 10. Normalized polarization-averaged absorption efficiency versus θ_{NW} and θ_{inc} for two different pitches ($P = 400$ and $500\,\text{nm}$). The black and red curves show the absorption efficiency for inclined InP NWs ($\varphi_{NW} = 0°$) as a function of θ_{NW} for normal incident light. The blue and green curves show the absorption efficiency versus θ_{inc} ($\varphi_{inc} = 0°$) for vertical NWs ($\theta_{NW} = 0°$, $\varphi_{NW} = 0°$). The diameter and length of the NWs are kept constant for all arrays ($D = 200\text{nm}$, $L = 1100\,\text{nm}$).

we considered InP NWs, but due to the generality of the models we expect the results to be valid also for other direct bandgap semiconductor systems.

Appendix

Fig. 9 shows polarization-averaged absorption spectra of inclined ($\theta_{NW} = 30°$) InP NWs versus azimuthal angle φ_{NW}. Varying φ_{NW} corresponds to rotating the NWs around the z axis (see schematics in Fig. 1). The results show that the absorption of light is nearly independent of φ_{NW}.

When $P = 400\,\text{nm}$, i.e., a smaller pitch than the $P = 500\,\text{nm}$ chosen in the main text, the absorption efficiency η increases (see Fig. 10). We assign this trend to an increasing amount of absorbing InP material in the NW array. However, due to absorption saturation, as also seen in Fig.

4, the peak in the absorption efficiency versus polar angle is less clear for $P = 400$ nm compared to $P = 500$ nm.

Acknowledgment

References

[1] W. Lu and C. M. Lieber, "Nanoelectronics from the bottom up," *Nat. Mater.*, vol. 6, pp. 841–850, 2007.
[2] X. Duan *et al.*, "Indium phosphide nanowires as building blocks for nanoscale electronic and optoelectronic devices," *Nature*, vol. 409, pp. 66–69, 2001.
[3] M. H. Huang *et al.*, "Room-temperature ultraviolet nanowire nanolasers," *Science*, vol. 292, pp. 1897–1899, 2001.
[4] J. Wang *et al.*, "Highly polarized photoluminescence and photodetection from single indium phosphide nanowires," *Science*, vol. 293, pp. 1455–1457, 2001.
[5] H. Pettersson *et al.*, "Infrared photodetectors in heterostructure nanowires," *Nano Lett.*, vol. 6, pp. 229–232, 2006.
[6] F. Patolsky and C. M. Lieber, "Nanowire nanosensors," *Mater. Today*, vol. 8, pp. 20–28, 2005.
[7] R. R. Lapierre, "Theoretical conversion efficiency of a two-junction III-V nanowire on Si solar cell," *J. Appl. Phys.*, vol. 110, 2011, Art. no. 014310.
[8] B. Tian *et al.*, "Coaxial silicon nanowires as solar cells and nanoelectronic power sources," *Nature*, vol. 449, pp. 885–889, 2007.
[9] G. Mariani *et al.*, "GaAs nanopillar-array solar cells employing in situ surface passivation," *Nat. Commun.*, vol. 4, 2013, Art. no. 1497.
[10] J. Wallentin *et al.*, "InP nanowire array solar cells achieving 13.8% efficiency by exceeding the ray optics limit," *Science*, vol. 339, pp. 1057–1060, 2013.
[11] I. Aberg *et al.*, "A GaAs nanowire array solar cell with 15.3% efficiency at 1 sun," *IEEE J. Photovolt.*, vol. 6, no. 1, pp. 185–190, Jan. 2016.
[12] B. Wang and P. W. Leu, "Tunable and selective resonant absorption in vertical nanowires," *Opt. Lett.*, vol. 37, pp. 3756–3758, 2012.
[13] K. Seo *et al.*, "Multicolored vertical silicon nanowires," *Nano Lett.*, vol. 11, pp. 1851–1856, 2011.
[14] L. A. Melnikov and E. A. Romanova, "Transformation of HE1m guided mode into the leaky one in absorbing optical fiber," *Opt. Commun.*, vol. 141, pp. 10–16, 1997.
[15] N. Anttu and H. Q. Xu, "Efficient light management in vertical nanowire arrays for photovoltaics," *Opt. Exp.*, vol. 21, pp. A558–A575, 2013.
[16] L. Cao *et al.*, "Engineering light absorption in semiconductor nanowire devices," *Nat. Mater.*, vol. 8, pp. 643–647, 2009.
[17] K. D. Song *et al.*, "Laterally assembled nanowires for ultrathin broadband solar absorbers," *Opt. Exp.*, vol. 22, pp. A992–A1000, 2014.
[18] Y. Yu *et al.*, "Dielectric core-shell optical antennas for strong solar absorption enhancement," *Nano Lett.*, vol. 12, pp. 3674–3681, 2012.
[19] Y. Yu and L. Cao, "Leaky mode engineering: A general design principle for dielectric optical antenna solar absorbers," *Opt. Commun.*, vol. 314, pp. 79–85, 2014.
[20] Z. Fan *et al.*, "Ordered arrays of dual-diameter nanopillars for maximized optical absorption," *Nano Lett.*, vol. 10, pp. 3823–3827, 2010.
[21] M. Aghaeipour *et al.*, "Tunable absorption resonances in the ultraviolet for InP nanowire arrays," *Opt. Exp.*, vol. 22, pp. 29204–29212, Nov. 2014.
[22] N. Anttu, "Geometrical optics, electrostatics, and nanophotonic resonances in absorbing nanowire arrays," *Opt. Lett.*, vol. 38, pp. 730–732, 2013.
[23] M. I. Kayes and P. W. Leu, "Comparative study of absorption in tilted silicon nanowire arrays for photovoltaics," *Nanoscale Res. Lett.*, vol. 9, 2014, Art. no. 620.
[24] Y. Wu *et al.*, "Enhanced photovoltaic performance of an inclined nanowire array solar cell," *Opt. Exp.*, vol. 23, pp. A1603–12, Nov. 2015.
[25] Y. Wang *et al.*, "Enhanced optical properties in inclined GaAs nanowire arrays for high-efficiency solar cells," *Opt. Laser Technol.*, vol. 85, pp. 85–90, 2016.
[26] G. Grzela *et al.*, "Nanowire antenna absorption probed with time-reversed Fourier microscopy," *Nano Lett.*, vol. 14, pp. 3227–3234, Jun. 2014.
[27] O. M. Ghahfarokhi *et al.*, "Performance of GaAs nanowire array solar cells for varying incidence angles," *IEEE J. Photovol.*, vol. 6, no. 6, pp. 1502–1508, Nov. 2016.
[28] V. Jain *et al.*, "Bias-dependent spectral tuning in InP nanowire-based photodetectors," *Nanotechnol.*, vol. 28, 2017, Art. no. 114006.
[29] D. R. Abujetas, R. Paniagua-Domínguez, and J. A. Sánchez-Gil, "Unraveling the Janus role of Mie resonances and leaky/guided modes in semiconductor nanowire absorption for enhanced light harvesting," *ACS Photon.*, vol. 2, pp. 921–929, 2015.
[30] C. Cheng and H. J. Fan, "Branched nanowires: Synthesis and energy applications," *Nano Today*, vol. 7, pp. 327–343, 2012.
[31] K. A. Dick *et al.*, "Growth of GaP nanotree structures by sequential seeding of 1D nanowires," *J. Cryst. Growth*, vol. 272, pp. 131–137, 2004.

[32] O. J. Glembocki and H. Piller, "Indium phosphide (InP)," in *Handbook of Optical Constants of Solids*, E. D. Palik, Ed. Burlington, NJ, USA: Academic, 1997, pp. 503–516.

[33] J. Li, H. Yu, and Y. Li, "Solar energy harnessing in hexagonally arranged Si nanowire arrays and effects of array symmetry on optical characteristics," *Nanotechnol.*, vol. 23, 2012, Art. no. 194010.

[34] H. Lu and C. Gang, "Analysis of optical absorption in silicon nanowire arrays for photovoltaic applications," *Nano Lett.*, vol. 7, pp. 3249–3252, 2007.

[35] [Online]. Available at: http://rredc.nrel.gov/solar/spectra/am1.5/

[36] M. Aghaeipour *et al.*, "Optical response of wurtzite and zinc blende gap nanowire arrays," *Opt. Exp.*, vol. 23, pp. 30177–30187, 2015.

[37] K. T. Fountaine, W. S. Whitney, and H. A. Atwater, "Resonant absorption in semiconductor nanowires and nanowire arrays: Relating leaky waveguide modes to Bloch photonic crystal modes," *J. Appl. Phys.*, vol. 116, 2014, Art. no. 153106.

[38] K. A. Dick *et al.*, "Improving InAs nanotree growth with composition-controlled Au-In nanoparticles," *Nanotechnol.*, vol. 17, pp. 1344–1350, 2006.

[39] K. A. Dick *et al.*, "The morphology of axial and branched nanowire heterostructures," *Nano Lett.*, vol. 7, pp. 1817–1822, 2007.